Faraday Rotation Measures in the parsec scale jets of the radio galaxies M87, 3C 111, and 3C 120

R. T. Zavala[1,2] & G. B. Taylor[1]

rzavala@nrao.edu, gtaylor@nrao.edu

Received _____; accepted _____

[1]National Radio Astronomy Observatory, P.O. Box 0, Socorro, NM 87801

[2]Department of Astronomy, New Mexico State University, MSC 4500 P.O. Box 30001, Las Cruces, NM 88003-8001

ABSTRACT

Parsec scale Faraday rotation measure maps are presented for the radio galaxies M87, 3C 111, and 3C 120. These VLBA observations were made at 8, 12, and 15 GHz. M87 has an extreme RM distribution which varies from -4000 rad m^{-2} to more than 9000 rad m^{-2} across a projected distance of 0.3 parsecs in its jet. M87 has no polarized flux closer than 17 mas from the core. 3C 111 and 3C 120 both show polarized emission in their cores which is consistent with the expectations of unified schemes for these broad line radio galaxies. 3C 111 has an RM gradient which increases from ~ -200 rad m^{-2} 4 mas from the core to ~ -750 rad m^{-2} on the side of the jet closest to the core. 3C 120 has a more moderate RM distribution in the jet of approximately 100 rad m^{-2} but this increases by an order of magnitude in the core. We find no detectable polarized emission from the radio galaxy J2022+616.

Subject headings: galaxies: active – galaxies: ISM – galaxies: individual(M87,3C 111,3C 111) – galaxies: jets – galaxies: nuclei – radio continuum: galaxies

1. Introduction

Several recent papers (Udomprasert et al. 1997, Cotton 1997 and Taylor 1998 & 2000) have demonstrated that extreme values of Faraday rotation of up to 40000 rad m^{-2} in the rest frame of quasars are possible. Zavala & Taylor (2001) showed that the Rotation Measure (RM) properties of quasars vary on both small spatial (parsec) scales and short timescales (1.5–3 years). These observations suggest that the observed RM distributions are intrinsic to the central few hundred parsecs of AGN and are not a foreground effect

from the host galaxy ISM, the ICM, or the Milky Way. Hence, the observed Faraday rotation can serve as a probe of the magnetic field weighted by the electron density along the line of sight near the central engines of AGN. With the electron density supplied by spectral line diagnostics (e.g. Osterbrock 1989) an estimate of the magnetic field strength and orientation can be made provided one assumes a physically reasonable path length.

To date parsec-scale RM observations have only been made for quasars. Polarimetric observations of other classes of AGN are required in order to test the unified model for AGN (Antonucci 1993) by looking for orientation effects in the RM distributions. In order to form a more complete picture of the parsec scale RM properties of AGN Taylor (2000) designed a sample of 40 quasars, BL Lacs, and radio galaxies for polarimetric observations. We have completed this survey with the VLBA and present here the first sub-parsec scale RM maps for radio galaxies.

In §2 we describe VLBA observations of the radio galaxies M87, 3C 111, 3C 120, and J2022+616 with the results of the rotation measure analysis presented in §3. In §4 we discuss our results in the light of unified schemes.

We assume $H_0 = 50$ km s^{-1} Mpc^{-1} and q_0=0.5 throughout.

2. Observations and Data Reduction

The observations, performed on 2000 June 27 (2000.40), were carried out at seven widely separated frequencies between 8.1 and 15.2 GHz using the 10 element VLBA[3]. Right- and left-circular polarizations were recorded using 1 bit sampling. The VLBA correlator

[3]The National Radio Astronomy Observatory is operated by Associated Universities, Inc., under cooperative agreement with the National Science Foundation.

produced 16 frequency channels across each IF during every 2 s integration.

Amplitude calibration and fringe-fitting were performed as in Taylor (2000). Feed polarizations of the antennas were determined using the AIPS task LPCAL. We assumed that the VLBA antennas had good-quality feeds with relatively pure polarizations, which allowed us to use a linearized model to fit the feed polarizations. This calibration was performed twice, first using J0136+478 with an accompanying CLEAN model for this polarized source. Plots of the real versus imaginary crosshand polarization data indicated that a satisfactory d-term solution was obtained. After this calibration was performed J2022+616 was found to be unpolarized. The d-terms were solved for again using J2022+616 as an unpolarized calibrator as a consistency check. Both sources produced nearly identical corrections for the d-terms, and J2022+616 was used as the final d-term calibrator.

Absolute electric vector position angle (EVPA) calibration was determined by using the EVPA's of J0854+201, J0927+390, J1310+323 and J2202+422 listed in the VLA Monitoring Program[4] (Taylor & Myers 2000). The EVPA calibration at 8 GHz was readily obtained from the polarization calibration website. The observations were interpolated in time as necessary. Polarization monitoring observations at 8 and 22 GHz were interpolated to produce position angles at 12 and 15 GHz. Figure 1 shows calibrated position angle results for these four calibrators with the associated VLA data from the website listed above. As a further test of our EVPA calibration we examined the rotation measure of component C4 of 3C 279 after the EVPA calibration was completed. In Zavala & Taylor (2001) C4 was shown to have a relatively low RM and $\chi = -84^{\circ}$ at 8 GHz to -87° at 15 GHz 2000 January 27. After the EVPA calibration for this experiment was completed we measured C4 and the EVPA was $-87°$ for all frequencies. Although component C4 does vary its position angle and RM with time the agreement between the observations of 2000

[4]http://www.aoc.nrao.edu/∼smyers/calibration/

January and 2000 July suggests that the polarization calibration was performed correctly.

To perform the rotation measure analysis data cubes in λ^2 were constructed. At 15 GHz the 4 IFs are adjacent and were thus combined to one data point at 15.165 GHz. The four IFs at 12 GHz were paired to produce measurements at 12.1 and 12.5 GHz. Separation of the four IFs at 8 GHz was sufficient to warrant their use as four individual data points for the RM analysis. There are then 7 points available to produce the RM fits with adequate short and long spacings in λ^2 to properly recover RMs between $\pm$ 30000 rad m^{-2}. The 12 and 15 GHz Stokes Q and U images used to produce the polarization angle maps were tapered to approximate the 8 GHz resolution, and a restoring beam matched to the 8 GHz beam was used.

3. Results

We present multifrequency radio observations, polarization properties, and rotation measure distributions for the radio galaxies M87, 3C 111, and 3C 120. No polarized flux was detected in J2022+616 at 15 GHz to a limit of percent polarization, m, of 0.1% in the core and 0.6% in the jet.

3.1. M87

This well studied galaxy was shown by Junor et al. (2001) to have an average RM of -4400 rad m^{-2} which varied from -2000 to -12000 rad m^{-2}. Our observations similarly show an extreme RM of -4830 ± 120 to $+9580 \pm 243$ rad m^{-2} 22$-$24 mas from the core (Fig. 2). This RM distribution is coincident with a peak in total intensity which appears displaced northward from the inner 15 mas of the jet. The RMs are mostly between -3000 and -5000 with the exception of a patch where the RMs increase in magnitude by a factor

two while changing sign to a positive slope. The sign change of the slope is significant, as it requires the magnetic field to change direction over a projected distance of 0.3 pc. Good agreement to the λ^2 signature of Faraday rotation is seen as indicated by the inset plots in Figure 2.

Although the significant polarized flux at 8 GHz is limited to the region of the RM signal there is some (4.5 ± 0.4 mJy) polarized emission at 15 GHz closer to the core. This occurs at ~ 17 mas from the core, in a *valley* of total intensity (at 15 GHz) between the inner jet and the displaced peak in I at 22−24 mas. The lack of corresponding polarized emission at 8 or 12 GHz is consistent with Faraday depolarization at lower frequencies if the RM gradient is greater than 2370 rad m^{-2} mas^{-1}.

3.2. 3C 111

This broad line radio galaxy (Sargent 1977) exhibits a gradient in RM towards the core. The RM changes from $\sim -208 \pm 45$ rad m^{-2} at 4 mas from the core to $\sim -734 \pm 58$ rad m^{-2} on the side of the jet closest to the core. As for M87, the polarized emission at 8 GHz for 3C 111 is limited to the region of the RM color overlay in Figure 3. However, significant polarized emission at 15 GHz (5.9 ± 0.4 mJy) exists within 2 mas of the core in 3C 111. At the location of the left-hand insert in Figure 3 the percent polarization is 12% at 15 GHz. The percent polarization 1.3 mas NE of the core is 1.5% at the same frequency.

3.3. 3C 120

3C 120 is another BLRG (Tadhunter et al. 1993) and its polarization properties were monitored over 16 months with the VLBA by Gómez et al. (2000). Gómez et al. (2000) reported an RM in the jet of 3C 120 of -6000 ± 2400 rad m^{-2} based on measurements

at 22 and 43 GHz. Our observation a little more than a year after Gómez et al shows a much smaller RM distribution. In Figure 4 it is apparent that 3C 120 has the lowest jet RM distribution of the three radio galaxies presented here, 108 ± 50 rad m^{-2}. The time variability of parsec scale RMs as seen in Zavala & Taylor (2001) is also present in 3C 120 (Gómez et al. 2000) and may account for the difference between our results and those of Gómez et al.

Contrary to M87 and 3C 111, 3C 120 has detectable polarized emission at all frequencies in the core and RMs of $|1000 - 2000|$ rad m^{-2} are present. As seen in Figure 4 the RM fits show considerable scatter at 8 GHz, and the reality of the sign change in the core RM distribution (from $+2000$ to -1000 rad m^{-2}) is suspect as the negative slope area shows deviations from a λ^2 law. The polarized flux within the core ranges from 4 ± 0.6 mJy at 8 GHz to $\sim 30 \pm 0.6$ mJy at 12 and 15 GHz. The range of m (15GHz) in the jet reach maxima of 9−16%, but within 1 mas from the center of the Stokes I image m falls to 3% or less.

4. Implications for Unified Schemes

Unified models for AGN describe radio galaxies as substantially inclined to the line of sight. This scenario places the core of a radio galaxy behind a dense multi-phase obscuring disk. The disk is expected to produce a high enough RM that the radio galaxy core is essentially unpolarized. Such a picture appears reasonable for M87, which is classified as a narrow line radio galaxy (Stauffer & Spinrad 1979 and Harms et al. 1994). This picture is supported by the lack of any polarized emission from the core of M87 (Figure 5). The requisite disk was first reported by Harms et al. (1994), although recent IR observations of M87 failed to detect the expected dust torus (Perlman et al. 2001). Even if the thick dust torus is absent a mechanism which accounts for the lack of polarized flux less than 17 mas

from the core is still required. Invoking a depolarizing Faraday screen requires such a screen to have a thickness of at least 3 parsecs. The RM data also require that the magnetic field be disordered on sub-parsec scales due to the sign change seen in the RM in Figure 1.

3C 111 and 3C 120 are classified as broad line radio galaxies and thus are expected to have jets more inclined towards the observer. Therefore, more polarized emission near the core might be expected as the central engine is uncovered by the obscuring torus. This is supported by the presence of polarized flux density at 15 GHz in the core for 3C 111 and at all three frequencies for 3C 120, consistent with their classification as BLRGs. Figure 5 illustrates this argument as both 3C 111 and 3C 120 have polarized emission at 15 GHz in their central regions.

Some caveats must be presented in this interpretation. Although M87 is classified as a NLRG, Sankrit, Sembach, & Canizares (1999) report that the Lymanα emission line has a width of 3000 km sec^{-1} which suggests that at least some of the broad line region is indeed visible. Using a black hole mass of 2.4 $\times 10^9$ M$_\odot$ (Harms et al. 1994) a velocity of 1860 km sec^{-1} is achieved at an orbital radius of 3 parsecs. Thus, the RM distribution observed in M87 may be produced by the broad line region itself. M87 is also a relatively low luminosity radio galaxy and may not provide a realistic comparison to more luminous objects. Lastly, the proximity of M87 also serves to expose details in its inner structure which may escape notice in 3C 111 and 3C 120 due to their greater distance.

5. Nature of the Faraday Screen

Given that Faraday rotation occurs, what part of the AGN plays the role of the Faraday screen? In Taylor (2000) this role was assigned to the narrow line region (NLR) itself, and the assumed properties of the NLR seemed consistent with the observed RMs.

However, the NLR is assumed to have a low volume filling factor ϵ (see Stauffer & Spinrad 1982 for M87 and Osterbrock & Miller 1975 for Cyg A). Taking a typical value for ϵ of 10^{-3} gives a covering factor of 0.01. Therefore, assuming a random distribution of NLR clouds, one should not expect the coherent RM distributions observed if only 1 percent of the beam is intersected the screen. Alternatively, the screen may consist of clouds which are entrained by the jet, perhaps in a boundary layer. This would account for the observed covering factor of the screen. A similar idea is put forth by Gómez et al. (2000) who propose a stationary cloud 0.4 pc across to explain the light curves and polarization properties of components in 3C 120.

To estimate a B field strength for a boundary layer screen in M87 we assume a scale size of 0.3 parsecs for clumps within the screen to match the scale size of the sign change of the RM slope. We use the electron density n_e of 1100 cm^{-3} from Stauffer & Spinrad (1982) to obtain a magnetic field strength of 16−34 μGauss. Such a field strength seems weak compared to Zeeman measurements in the center of our own galaxy of 0.5 mG (Crutcher et al. 1996) to 3 mG (Plante et al. 1995). If the magnetic field is in equilibrium with a gas at a temperature of 10^4K and using the electron density of Stauffer & Spinrad (1982) a magnetic field strength of 200μGauss is obtained.

The presence of broad Lyα lines in M87 prompts consideration of the BLR as a Faraday screen. As discussed in §4 the observed Lyα velocity could be found within 3 parsecs of the black hole, placing the Lyα clouds along the line of sight to the jet in our VLBA images. However, the free-free opacity at the expected n_e of 10^{10} cm^{-3} (Matthews & Capriotti 1985) makes the BLR clouds optically thick at 8−15 GHz (Marscher & Brown 1975).

Lastly, we consider the hot, tenuous gas that is expected to confine the NLR clouds. Such a gas is expected to be disordered and radiation propagating through it should experience a random walk RM effect. This would produce an RM with a zero mean,

Gaussian distribution. Such a distribution is definitely lacking for M87 and 3C 111, and possibly for 3C 120 as well. Without tighter constraints on the physical parameters it is not possible to discriminate between these, or other, Faraday screen scenarios.

We thank Avi Loeb for pointing out the possible significance of the broad line region in the RM distribution of M87. This research has made use of the NASA/IPAC Extragalactic Database (NED) which is operated by the Jet Propulsion Laboratory, Caltech, under contract with NASA. This research has made use of NASA's Astrophysics Data System Abstract Service. RTZ gratefully acknowledges support from NRAO for a pre-doctoral research position.

REFERENCES

Antonucci, R. 1993, ARA&A, 31, 473

Cotton, W. D., Dallacasa, D., Fanti, C., Fanti, R., Foley, A. R., Schilizzi, R. T., & Spencer, R. E. 1997, A&A, 325, 493

Crutcher, R. M., Roberts, D. A., Mehringer, D. M., & Troland, T. H. 1996, ApJ, 462, 79

Gómez, J. ;., Marscher, A. P., Alberdi, A., Jorstad, S. G., & García-Miró, C. 2000, Science, 289, 2317

Harms, R. J. et al. 1994, ApJ, 435, L35

Junor, W., Biretta, J. A., & Wardle, J. F. C. 2001, in IAU Symposium 25, Galaxies and their constituents at the highest angular resolutions, ed. R. T. Schilizzi, S. N. Vogel, F. Paresce & M. S. Elvis (San Francisco:ASP) 136

Marscher, A. P. & Brown, R. L. ApJ, 483, L9

Matthews, W. G. & Capriotti, E. R. 1985, in Astrophysics of active galaxies and quasi-stellar objects. ed. J. S. Miller (Mill Valley:University Science Books)

Osterbrock, D. E. 1989, Astrophysics of Gaseous Nebulae and Active Galactic Nuclei (Mill Valley: University Science Books)

Perlman, E. S., Sparks, W. B., Radomski, J., Packham, C., Fisher, R. S., Piña, R., & Biretta, J. A. 2001, ApJ, 561, L51

Plante. R. L., Lo, K. Y., & Crutcher, R. M. 1995, ApJ, 445, L113

Sankrit, R., Sembach, K. R., & Canizares, C. R. 1999, ApJ, 527, 733

Sargent, W. L. W. 1977, ApJ, 212, L105

Stauffer, J. & Spinrad, H. 1979, ApJ, 231, L51

Tadhunter, C. N., Morganti, R., di Serego-Alighieri, S., Fosbury, R. A. E., & Danziger, I. J. 1993, MNRAS, 263, 999

Taylor, G. B. 1998, ApJ, 506, 637

Taylor, G. B. 2000, ApJ, 533, 95

Taylor, G. B. & Myers, S. T. 2000 VLBA Scientific Memo 26, National Radio Astronomy Observatory

Udomprasert, P. S., Taylor, G. B., Pearson, T. J., & Roberts, D. H. 1997, ApJ, 483, L9

Zavala, R. T. & Taylor, G. B. ApJ, 550, L147

This manuscript was prepared with the AAS LaTeX macros v5.0.

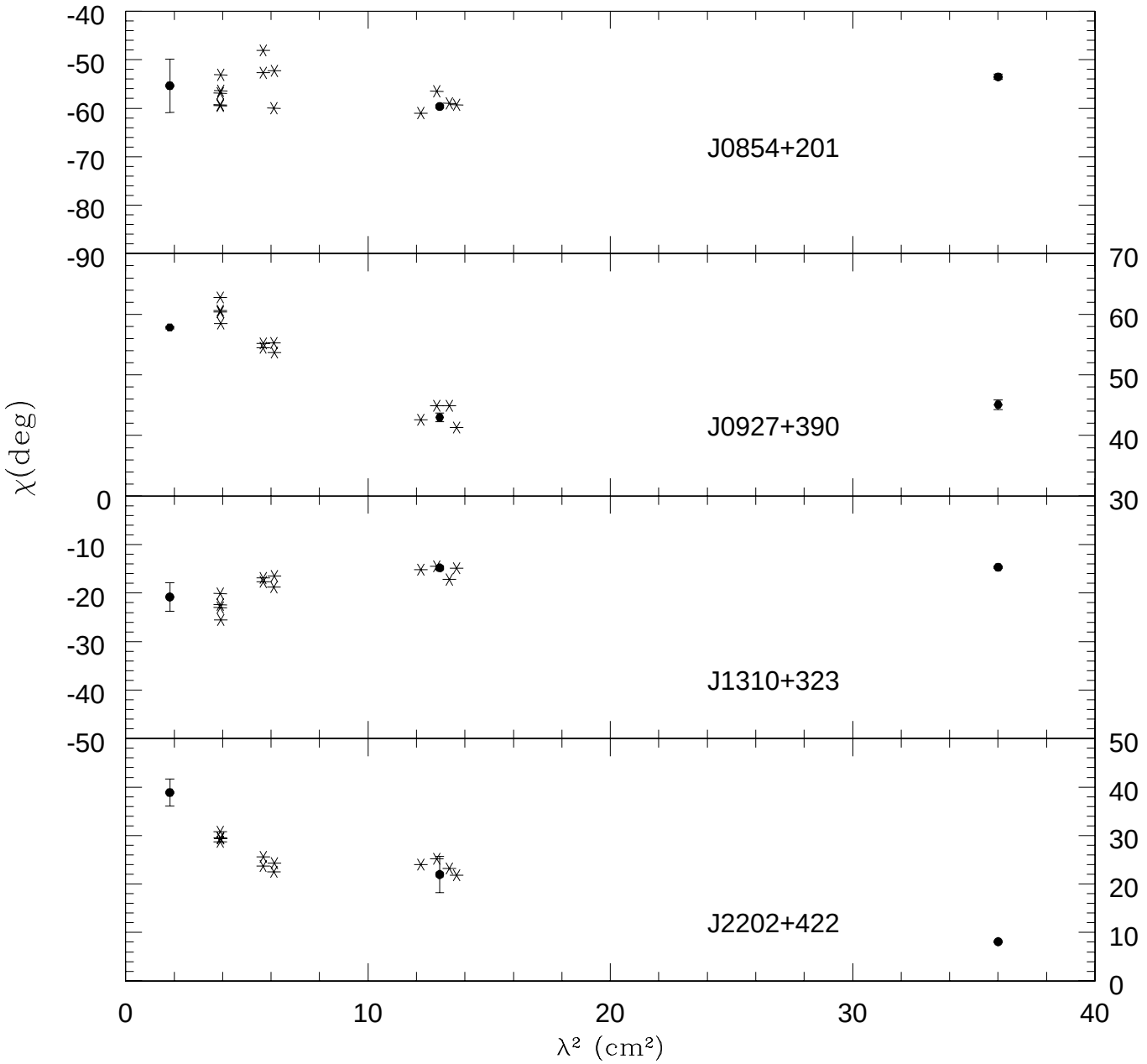

Fig. 1.— Plot of EVPA vs. λ^2 for calibrators listed in §2. Asterisks are EVPA after applying correction based on VLA polarization monitoring data. Filled circles represent VLA polarization monitoring data for the calibrators. A single date indicates the date of observation from the VLA polarization monitoring data. If two dates are shown the VLA data was interpolated between those dates to produce the plot. Uncertainty in position angle is estimated as $\pm 5^{o}$ for all frequencies after EVPA calibration.

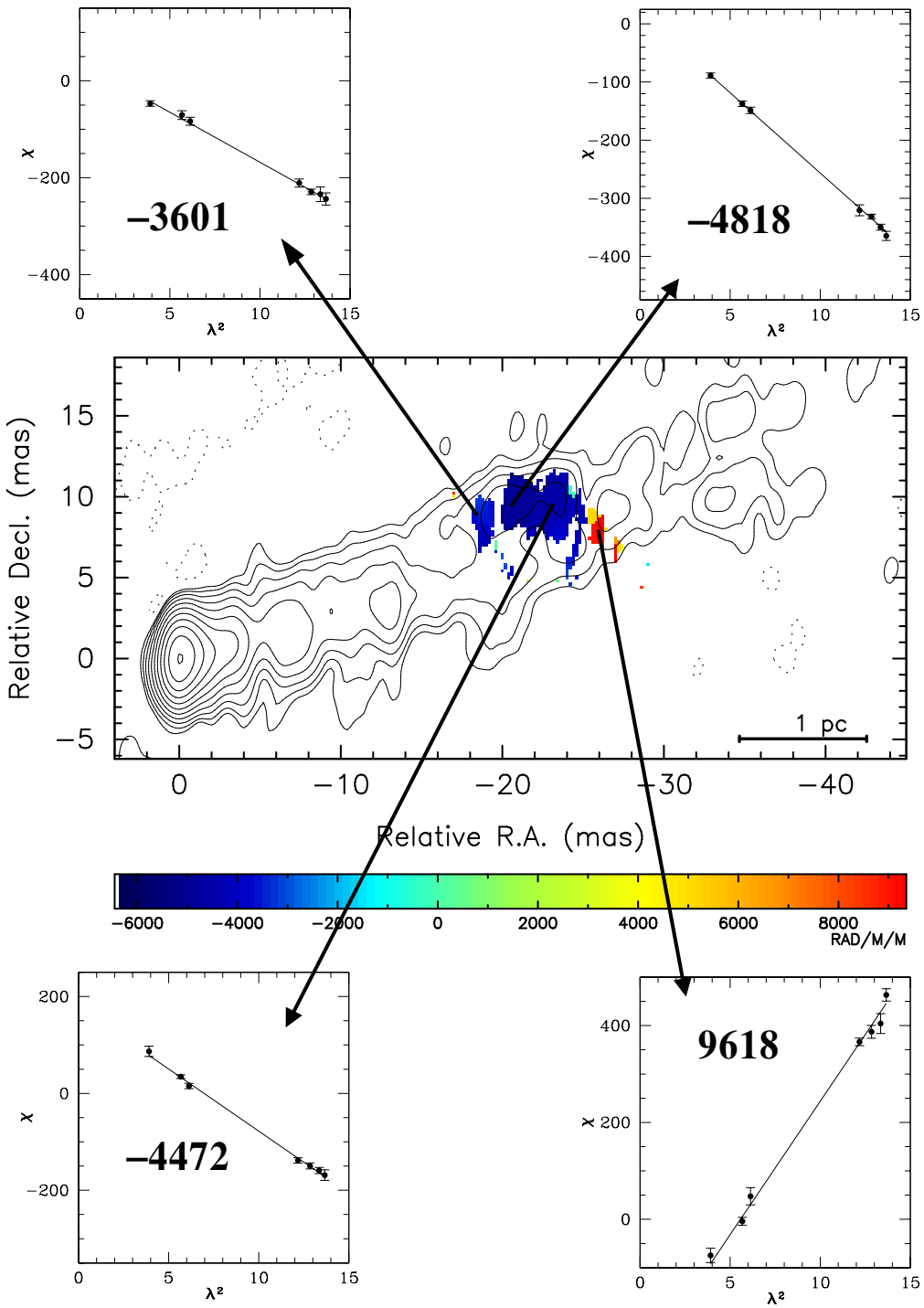

Fig. 2.— Rotation measure image of M87 from data at 8 to 15 GHz, with contours of total intensity at 8 GHz overlaid. The restoring beam has dimensions 1.1 × 2.1 milliarcsec at position angle 0°. The colorbar ranges from −1500 to +300 rad m^{-2} . Contours start at 1 mJy/beam and increase by factors of 2.

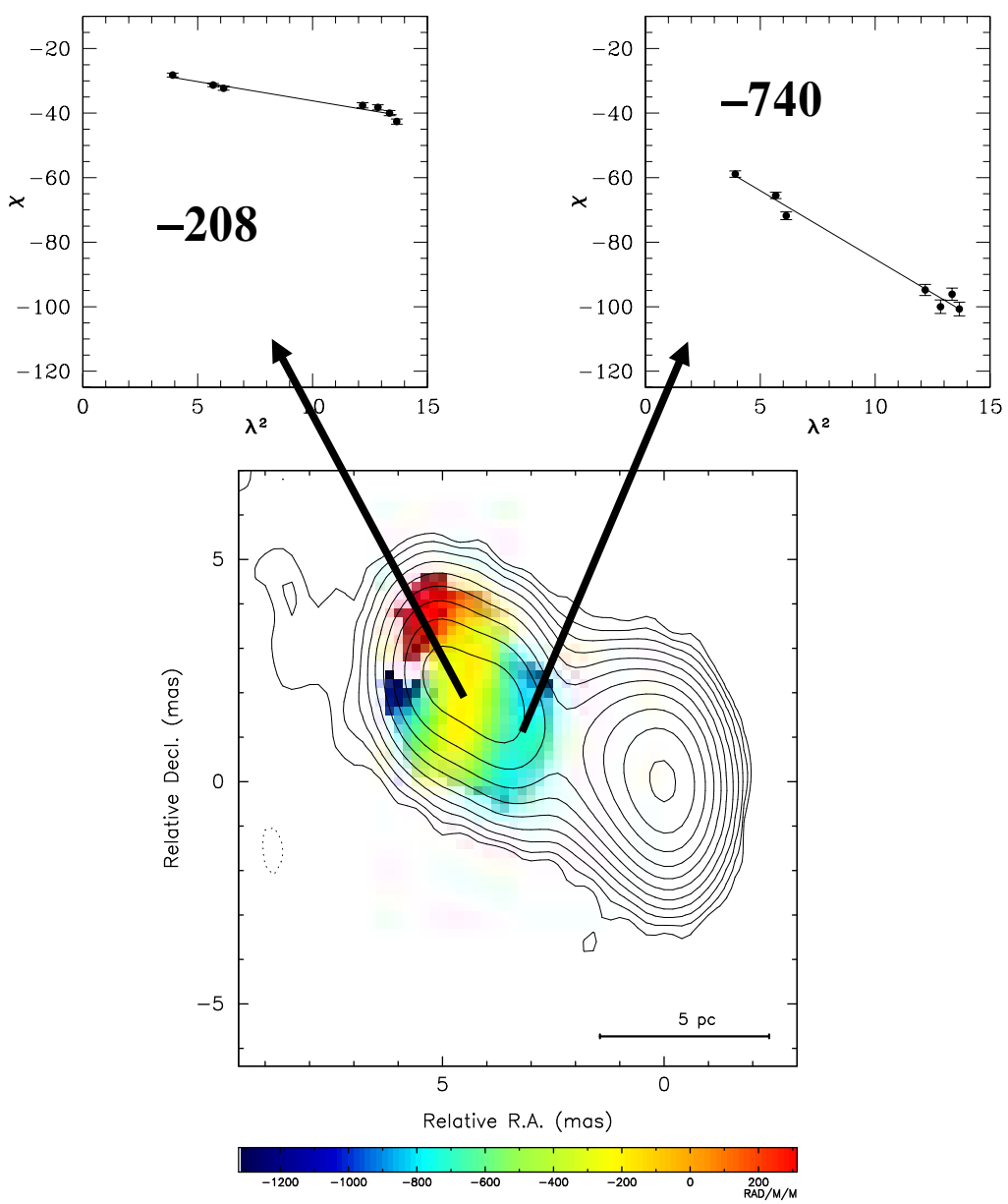

Fig. 3.— Rotation measure image of 3C 111 from data at 8 to 15 GHz, with contours of total intensity at 8 GHz overlaid. The insets display rotation measure fits at the points indicated in rad m^{-2}. The restoring beam has dimensions of 0.6 × 1.2 milliarcsec at position angle 0°. The colorbar ranges from −4400 to +2650 rad m^{-2}. Contours start at 0.75 mJy/beam and increase by factors of 2.

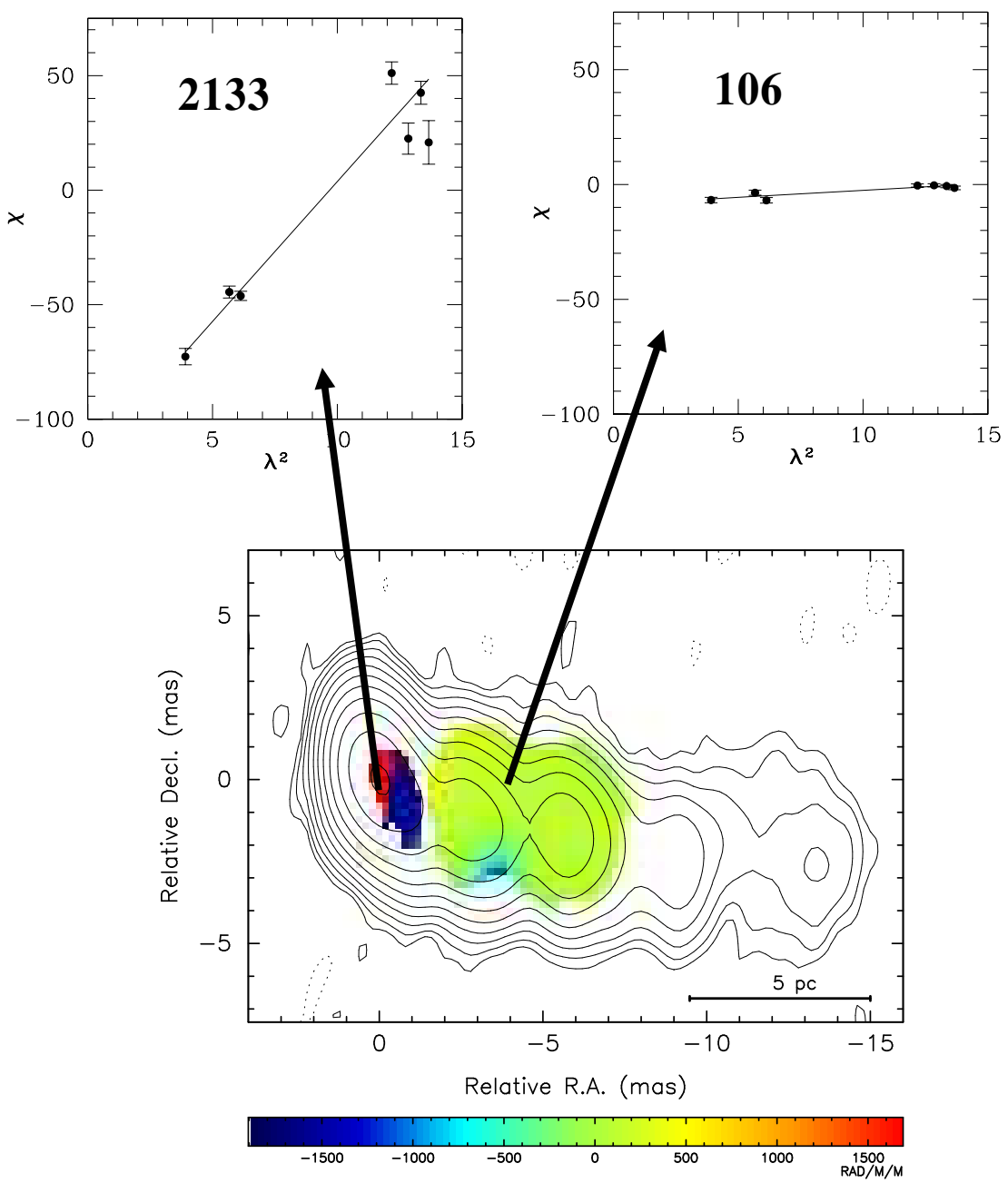

Fig. 4.— Rotation measure image of 3C 120 from data at 8 to 15 GHz, with contours of total intensity at 15 GHz overlaid. The insets display rotation measure fits at the points indicated in rad m^{-2}. The restoring beam has dimensions 1.0 × 2.5 milliarcsec at position angle 0°. The colorbar ranges from −3000 to +2100 rad m^{-2}. Contours start at 1 mJy/beam and increase by factors of 2.

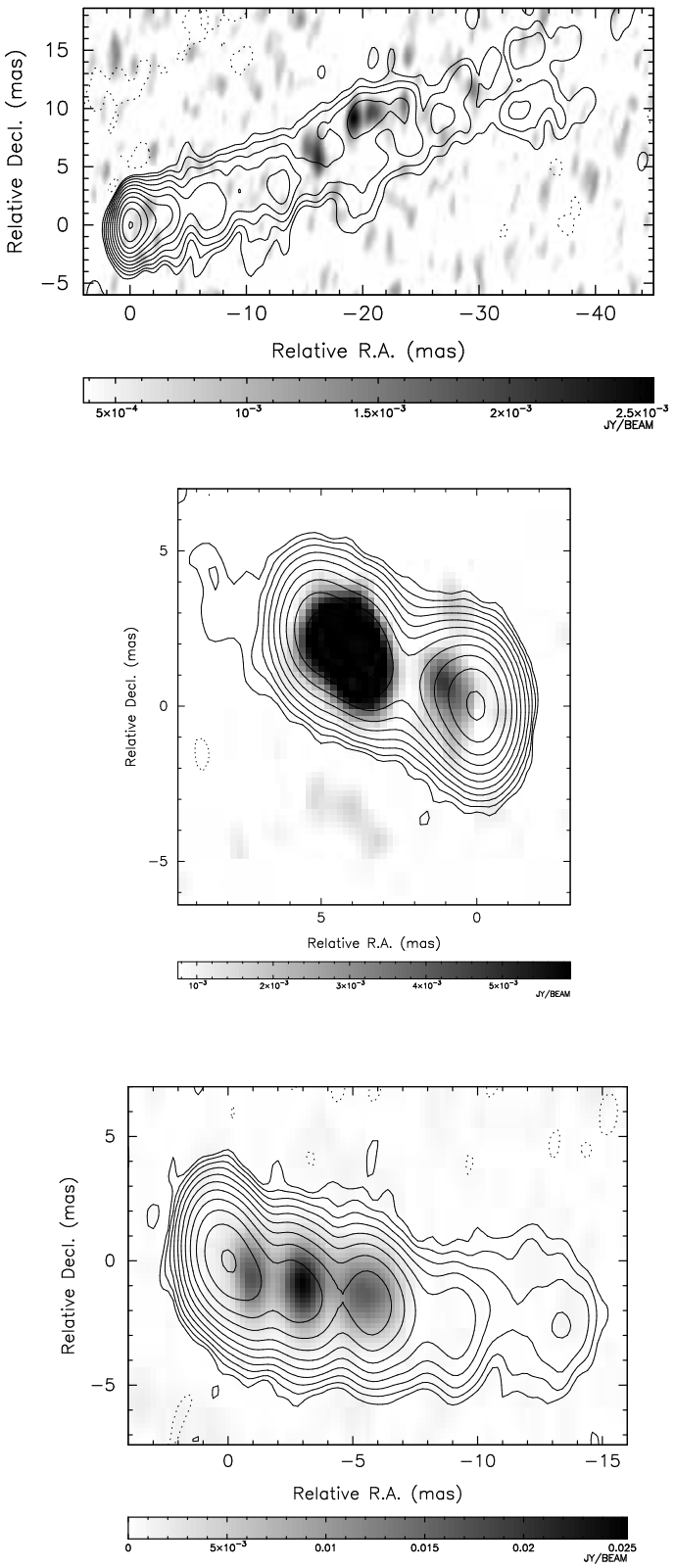

Fig. 5.— Mosaic of 8 GHz total intensity (contours) with 15 GHz polarized intensity (greyscale) overlaid. The contours are the same as for Figures 2-5.